ISSN 1674-1056
http://cpb.iphy.ac.cn
http://iopscience.iop.org/cpb
中国物理 B
Chinese Physics
中国物理
Chinese Physics B

Single-electron transport through single and coupling dopant atoms in silicon junctionless nanowire transistor

Xiao-Di Zhang(张晓迪)[1,2], Wei-Hua Han(韩伟华)[1,2], Wen Liu(刘雯)[1,2], Xiao-Song Zhao(赵晓松)[1,2], Yang-Yan Guo(郭仰岩)[1,2], Chong Yang(杨冲)[1,2], Jun-Dong Chen(陈俊东)[1,2], Fu-Hua Yang(杨富华)[1,2,3]

Citation: Chin. Phys. B . 2019, 28(12): 127302 . **doi:** 10.1088/1674-1056/ab527a
Journal homepage: http://cpb.iphy.ac.cn; http://iopscience.iop.org/cpb

What follows is a list of articles you may be interested in

Observation of hopping transitions for delocalized electrons by temperature-dependent conductance in siliconjunctionless nanowire transistors

Yang-Yan Guo(郭仰岩), Wei-Hua Han(韩伟华), Xiao-Song Zhao(赵晓松), Ya-Mei Dou(窦亚梅), Xiao-Di Zhang(张晓迪), Xin-Yu Wu(吴歆宇), Fu-Hua Yang(杨富华)

Chin. Phys. B . 2019, 28(10): 107303 . **doi:** 10.1088/1674-1056/ab3e68

Multi-step shot noise spectrum induced by a local large spin

Niu Peng-Bin, Shi Yun-Long, Sun Zhu, Nie Yi-Hang

Chin. Phys. B . 2015, 24(12): 127309 . **doi:** 10.1088/1674-1056/24/12/127309

Two-electron localization in a quantum dot molecule driven by a cosine squared field

Zhong Guang-Hui, Wang Li-Min

Chin. Phys. B . 2015, 24(4): 047306 . **doi:** 10.1088/1674-1056/24/4/047306

Fano-type resonances induced by a boson mode in Andreev conductance

J. Barański, T. Domański

Chin. Phys. B . 2015, 24(1): 017304 . **doi:** 10.1088/1674-1056/24/1/017304

Temperature-controllable spin-polarized current and spin polarization in a Rashba three-terminal double-quantum-dot device

Hong Xue-Kun, Yang Xi-Feng, Feng Jin-Fu, Liu Yu-Shen

Chin. Phys. B . 2013, 22(5): 057306 . **doi:** 10.1088/1674-1056/22/5/057306

Single-electron transport through single and coupling dopant atoms in silicon junctionless nanowire transistor*

Xiao-Di Zhang(张晓迪)[1,2], Wei-Hua Han(韩伟华)[1,2,†], Wen Liu(刘雯)[1,2], Xiao-Song Zhao(赵晓松)[1,2], Yang-Yan Guo(郭仰岩)[1,2], Chong Yang(杨冲)[1,2], Jun-Dong Chen(陈俊东)[1,2], and Fu-Hua Yang(杨富华)[1,2,3]

[1] *Engineering Research Center for Semiconductor Integrated Technology & Beijing Engineering Center of Semiconductor Micro-Nano Integrated Technology, Institute of Semiconductors, Chinese Academy of Sciences, Beijing* 100083, *China*

[2] *Center of Materials Science and Optoelectronics Engineering, University of Chinese Academy of Sciences, Beijing* 100049, *China*

[3] *State Key Laboratory for Superlattices and Microstructures, Institute of Semiconductors, Chinese Academy of Sciences, Beijing* 100083, *China*

(Received 16 September 2019; revised manuscript received 28 October 2019; published online 15 November 2019)

We investigated single-electron tunneling through single and coupling dopant-induced quantum dots (QDs) in silicon junctionless nanowire transistor (JNT) by varying temperatures and bias voltages. We observed that two possible charge states of the isolated QD confined in the axis of the initial narrowest channel are successively occupied as the temperature increases above 30 K. The resonance states of the double single-electron peaks emerge below the Hubbard band, at which several subpeaks are clearly observed respectively in the double oscillated current peaks due to the coupling of the QDs in the atomic scale channel. The electric field of bias voltage between the source and the drain could remarkably enhance the tunneling possibility of the single-electron current and the coupling strength of several dopant atoms. This finding demonstrates that silicon JNTs are the promising potential candidates to realize the single dopant atom transistors operating at room temperature.

Keywords: silicon nanowire transistor, single electron tunneling, dopant-induced quantum dots, tunneling current spectroscopy

PACS: 73.63.Kv, 73.23.Hk, 73.43.Jn, 85.35.Gv **DOI:** 10.1088/1674-1056/ab527a

1. Introduction

Single electron transport through the dopant-induced quantum dots (QDs) in silicon nanoscale transistors is attractive for future quantum computing since it would allow a low-power dissipation and high packing density.[1] In conventional devices, the main role of dopants is to provide carriers because of their relatively shallow ground-state energy level, e.g., 45 meV for phosphorus. Beyond this main function, the ionized dopant atoms can further work as QDs when they are embedded in a nanostructured channel, where the ionization energy of the dopant atom is larger than that of bulk silicon due to quantum confinement and dielectric confinement.[2,3] In recent years, a silicon nano-transistor with a few donor atoms has been reported to work at room temperature since the ground state energy level is significantly deepened due to the dopant atom coupling by applying selective-doping technique to extremely narrow and thin silicon nanowires.[4] The ensemble of the donors in the slit channel possibly enhances the dielectric confinement due to the created polarization charges at the interface between the silicon channel and its surrounding dielectric layer.[5] The enhanced ionization energy for the dopants close to the interface is inversely proportional to the distance from the dielectric interface.[6] As a result, the ionization energy increases with decreasing nanowire radius, which can significantly reduce the carrier density below the radius of 10 nm.[7] However, it is still a great challenge to control the position and the number of individual dopant atoms in an ultra-narrow silicon channel. Silicon junctionless nanowire transistor (JNT) as a gated resistor is an alternative choice because of its adjustable conduction radius in the axis of the silicon nanowire, which is controlled by the gate voltages.[8] The channel of JNT has the same doping type and concentration as the drain and the source. The whole channel is fully depleted in the off state, while the channel is broadened gradually with the gate voltage increasing. It might be found that the single-electron tunnels through a single dopant-induced quantum dot, which is strongly confined in the axis of the initial narrowest channel. With further broadening of the channel, several ionized dopant atoms are coupled together in a longer chain, which develops the up and down spin states of each dopant atom into upper and lower Hubbard bands.[9]

In the present work, we investigate single electron tunneling through single and coupling dopant-induced QDs confined strongly in the axis of the silicon JNT channel by varying the temperatures and bias voltages. Double current peaks of single electron tunneling are observed subsequently at the initial stage of the gate-voltage dependent current spectrum with the temperature increasing from 6 K to 70 K. The double isolated current peaks are attributed to electrons occupying the two energy states of a single dopant-induced QD. The isolated

*Project supported by the National Key R&D Program of China (Grant No. 2016YFA0200503).

†Corresponding author. E-mail: weihua@semi.ac.cn

© 2019 Chinese Physical Society and IOP Publishing Ltd

single-electron peaks emerge below the lower Hubbard band, at which several subpeaks are clearly observed separately in the double oscillated current peaks due to the coupling of QDs. The electric field of bias voltage V_d between the source and the drain could remarkably enhance the tunneling possibility of the single-electron current and the coupling strength of several dopant atoms at the low temperatures.

2. Experiment

We fabricated a heavily n-doped JNT on a (100)-oriented silicon-on-insulator (SOI) wafer, whose top silicon layer with the thickness of 55 nm on a buried oxide layer of 145 nm was implanted by the phosphorus ions with a dose of 5×10^{13} cm^{-2}. The $\langle 110\rangle$ oriented silicon nanowire was defined by electron beam lithography (EBL) and inductively coupled plasma (ICP) etching. The effective section size of the silicon nanowire is estimated to be 27 nm×30 nm after the process of sacrificial oxidation in the 5% HF and thermal oxidation in dry oxygen at 900 °C for 1 h for 22-nm gate dielectric layer. After 200-nm-thick polysilicon layer was deposited by low pressure chemical vapor deposition (LPCVD), the 280 nm-long gate was defined by EBL and ICP, as shown in the top view of the scanning electron microscope (SEM) image in Fig. 1(a). Finally, the source, drain, and gate electrodes were fabricated by Ni/Si ohmic contact and Al metallization. The schematic structure of JNT is shown in Fig. 1(b). The characterizations of drain current were measured by Agilent B1500A semiconductor parameter analyzer within the temperature range from 6 K to 70 K.

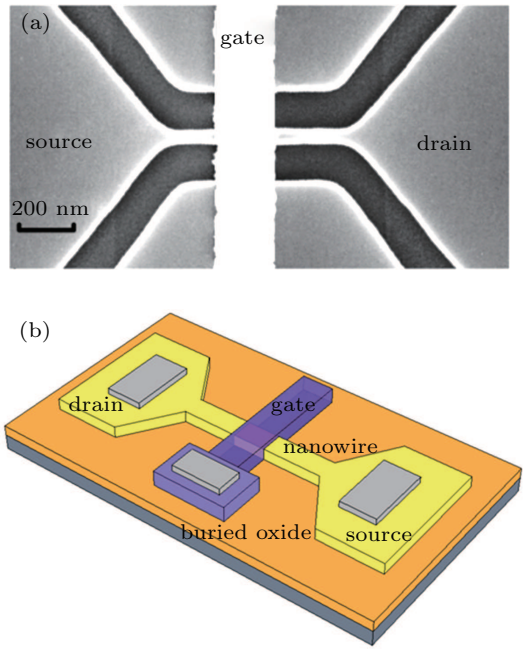


Fig. 1. (a) The top view of SEM image for JNT after deposition of 280 nm-long polysilicon gate. (b) Structural diagram of JNT device.

3. Results and discussion

The drain current I_d was measured as a function of the gate voltage V_g at different temperatures. Figure 2(a) shows the gate voltage dependence of the drain current at the bias V_d of 10 mV within the temperature range from 6 K to 70 K. At the initial stage of the transfer characteristics, we can firstly observe a remarkable isolated current peak at the gate voltage of 1.19 V which appears below two oscillated current peaks at the temperatures of lower than 30 K. With the temperature increasing, the second isolated current peak successively emerges at the gate voltage of 1.03 V. Doubles of the isolated current peaks and oscillated current peaks are marked by four blue arrows, which indicate that the peak positions are stable with varying temperatures respectively at the gate voltages of 1.07 V, 1.19 V, 1.36 V, and 1.64 V. It is easy to understand that the discrete dopant atom is strongly confined in the axis of the initial narrowest channel at the initial stage of transfer characteristic. With the gate voltage increasing, several ionized dopant atoms are coupled together in a longer chain as the channel is broadened gradually. The inset of Fig. 2(a) presents the measured stability diagram of drain current I_d versus gate and bias voltages at the temperature of 6 K, in which we can easily find two Coulomb diamond regions for the gate voltage $V_g \approx 1.25$–1.9 V. The same positive and negative slopes in the two Coulomb diamond regions indicate that there are stable capacitances C_s, C_d, and C_g between the coupling dopant atoms and the source, drain, and gate electrodes, respectively. We may further find the conducting region with steeper slopes for a discrete dopant-induced QD at the gate voltage $V_g \approx 1.0$–1.25 V in the inset of Fig. 2(c) if focusing on the current range less than 0.06 nA for the stability diagram in the inset of Fig. 2(a). As a result, the double isolated current peaks would be related to single electron tunneling through the two energy states of a single dopant-induced QD with the Fermi energy level moving up. The oscillated peaks with several subpeaks come from the coupling of several dopant-induced QDs within the broadening channel.

In order to clearly observe the electron transport behaviors, we extracted the transconductance g_m curves in Fig. 2(b) from the transfer characteristics in Fig. 2(a). With the increase of temperature, the subpeaks in the oscillated g_m peaks are gradually smooth out but the isolated current peaks are enhanced significantly at the resonant levels. The result indicates that the thermal energy could enhance the probability of electron tunneling and the coupling of the dopant atom array.[10] At the temperature of 70 K, the g_m peak positions are located respectively at the gate voltages of 1.043 V, 1.163 V, 1.275 V, and 1.558 V. The gate spacing ΔV_{g1} of the double isolated g_m peaks can be measured to be about 120 mV. According to single electron tunneling, the self-gate capacitance C_{g1} for a dopant-induced QD is determined to be 1.33 aF by

$C_{g1} = e/\Delta V_{g1}$. The radius r of the QD is estimated to be about 1.02 nm according to $C_{g1} = 4\pi\varepsilon_0\varepsilon_r r$. However, the gate spacing ΔV_{g2} of the double oscillated g_m peaks is enhanced to be about 283 mV. The self-gate capacitance C_{g2} for the coupling dopant-induced QD array would change to be 0.56 aF according to $C_{g2} = e/\Delta V_{g2}$. The energy change is related to the gate conversion factor $\alpha = C_g/(C_g + C_s + C_d)$ and the gate spacing ΔV_g of the g_m peaks, i.e., $\Delta E = e\alpha\Delta V_g$.[11] Here, we define the total capacitance $C_\Sigma = C_g + C_s + C_d$. The factor α can be estimated by the positive and negative slopes of the Coulomb diamond regions, which equal to $C_g/(C_g + C_d)$ and C_g/C_s. According to the stability diagram for an isolated current peak in the inset of Fig. 2(c), the factor α_1 is calculated to be 0.112 by measured steeper slopes $C_{g1}/(C_{g1} + C_d) = 0.192$ and $C_{g1}/C_s = 0.27$. Then, the energy spacing of the double isolated g_m peaks is calculated to be 13.44 meV. According to the stability diagram for the oscillated current peaks in the inset of Fig. 2(a), the factor α_2 is calculated to be 0.047 by diamond slopes $C_{g2}/(C_{g2} + C_d) = 0.0948$ and $C_{g2}/C_s = 0.0934$. Then, the energy spacing of the double oscillated g_m peaks is obtained to be 13.31 meV. The results indicate that the energy spacing in the coupling QD array is similar to that of a single QD. In order to understand the results, we find that the total capacitances C_Σ for the single QD and the coupling QDs are basically the same according to the calculation of $C_{g1}/\alpha_1 = 11.875$ aF and $C_{g2}/\alpha_2 = 11.915$ aF. As a result, the charge energy $U = e^2/C_\Sigma$ that dominates the energy spacing would be stable at about 13.4 meV even though the gate voltage is increased.

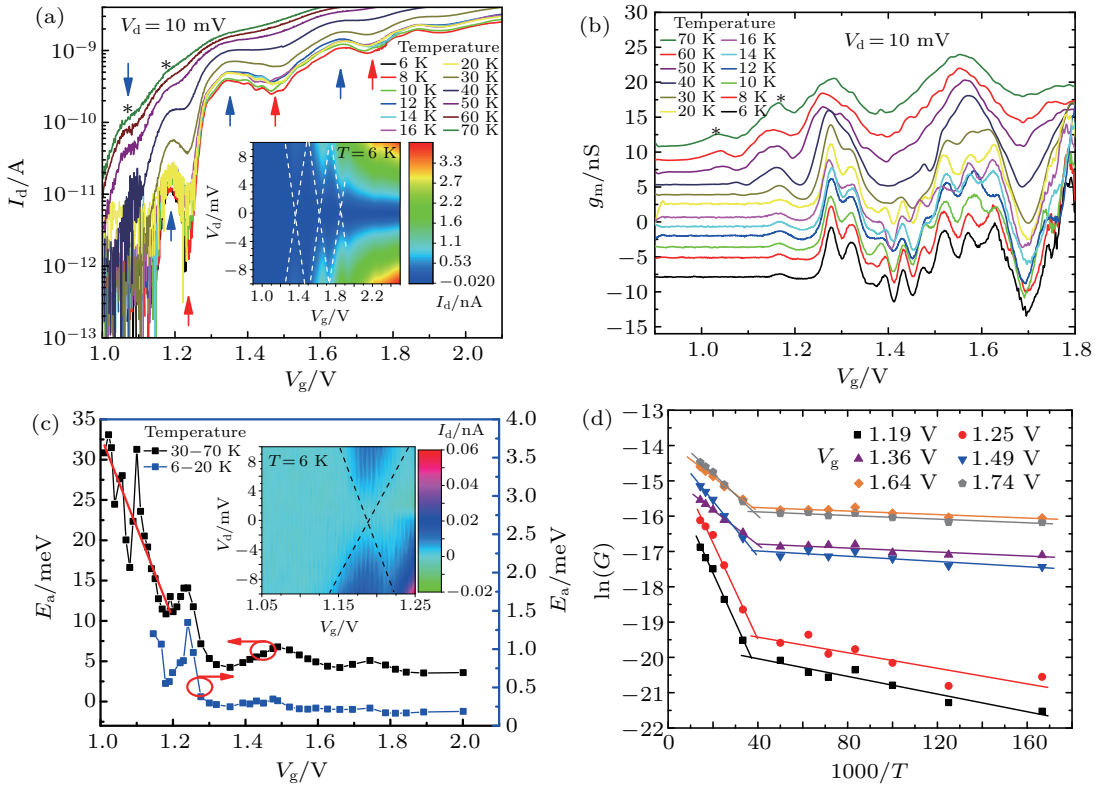


Fig. 2. (a) Temperature dependence of I_d–V_g characteristics ($V_d = 10$ mV) for silicon JNT (6–70 K). Inset: stability diagram of drain current I_d vs. gate and bias voltages at $T = 6$ K. (b) The transconductance g_m versus gate voltage V_g with $V_d = 10$ mV from 6 K to 70 K. The transconductance curves have been shifted by an offset 2 nS for clarity. (c) Activation energy E_a estimated from Arrhenius plots as a function of V_g at $V_d = 10$ mV in two different temperature regions. Inset: the current range narrowed less than 0.06 nA for the stability diagram in the inset of (a) for clarify at the low V_g. (d) The Arrhenius plots of conductance at various gate voltages corresponding to the marked V_g by arrows in (a).

The tunneling barrier for the confinement of dopant-induced QDs is dependent on the gate voltages.[12] Figure 2(c) presents the gate-dependent thermal activation energy E_a for electrons tunneling within different temperature ranges of 30–70 K and 6–20 K. The data of E_a are extracted from the slope of the Arrhenius plots in Fig. 2(d). Here, we only present the temperature-dependent data of the conductance peaks and valleys. The temperature-dependent conductance G follows the model

$$G = G_0 \exp(-E_a/k_B T), \quad (1)$$

where k_B is the Boltzmann's constant and E_a represents the activation energy.[13] The activation energy E_a has the minima at the current peak positions and the maxima at the current valley positions. Within the higher temperature range of 30–70 K, the linear dependence of the activation energy shows a good gate conversion factor $\alpha = 0.113$ for the gate voltage range from 1.0 V to 1.25 V, in which the tunneling barrier height is modulated linearly for an isolated dopant-induced QD by the gate voltage. The activation energies below the gate voltage of 1.19 V, at which there emerges the first isolated current peak,

are not less than the charging energy of 13.4 meV basically. With the gate voltage increasing from 1.3 V to 1.9 V, the activation energies for electron hopping through the coupling QD array are reduced to be about 3.5–6.8 meV, which is close to the thermal energy k_BT. Such activation energies for electron hopping are equivalent to the mean of the energy interval between neighbor coupling QDs. Therefore, the electron transport is dominated by thermally activated hopping within the higher temperature range of 30–70 K. However, at the lower temperature range of 6–20 K, the activation energies are reduced to be 0.5–1.5 meV from the first current peak to valley at the gate voltage $V_g = 1.15$–1.25 V. With the gate voltage increasing, the activation energies for the coupling QD array are rapidly reduced to be 0.2–0.3 meV. In this case, the tunneling electrons would find the similar energy states between the coupling QDs by the variable range hopping around Fermi level. Therefore, the electron transport is dominated by the tunneling in the lower temperature range of 6–20 K.

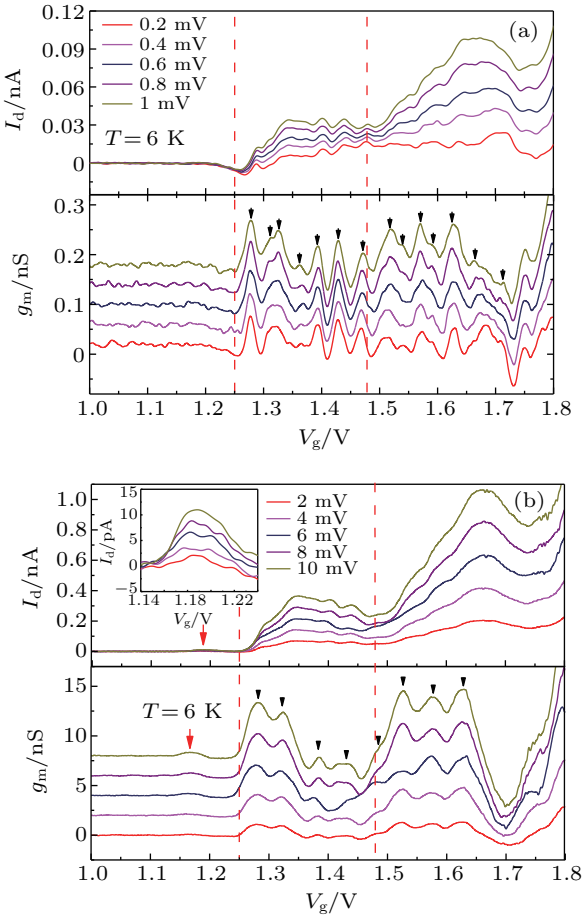


Fig. 3. (a) The I_d–V_g and g_m–V_g characteristics of the device at $T = 6$ K by varying the bias V_d from 0.2 mV to 1.0 mV with the step of 0.2 mV. (b) I_d–V_g and and g_m–V_g curves of the device at $T = 6$ K by varying the bias V_d from 2 mV to 10 mV.

In order to further understand the emergence of isolated current peaks, we measured the transfer characteristics I_d–V_g and g_m–V_g of the device at the temperature of 6 K by varying the bias V_d from 0.2 mV to 1.0 mV with the step of 0.2 mV, as shown in Fig. 3(a). The seven subpeaks are clearly observed separately in the double oscillated current peaks due to coupling QDs, by which electron tunneling can mix single QD states to form upper and lower Hubbard bands. The subpeak spacing is about 32.3 mV, which corresponds to the coupling energy of 1.45 meV. Interestingly, the coupling energy is comparative to the activation energy for hopping electrons at the gate voltage of 1.25 V in lower temperature ranges in Fig. 2(c), which are blockaded in the current valley. However, there is no isolated single-electron peak below the lower Hubbard band as the bias voltage is less than 1.0 mV. Figure 3(b) further provides the double oscillated current peaks in the I_d–V_g curves of the device at the temperature of 6 K by improving the bias V_d from 2 mV to 10 mV with the step of 2 mV. It is clearly observed in the inset of Fig. 3(b) that the first single-electron current peak at the gate voltage of 1.185 V is enhanced in amplitude with the bias voltage increasing. Since the potential difference between the source and the drain is increased by the bias voltage, only four subpeaks are clearly observed separately in the double oscillated current peak. The subpeak spacing is enhanced to be about 48.7 mV, corresponding to the coupling energy of 2.2 meV. Thus, the electric field of bias voltage V_d between the source and the drain could remarkably enhance not only the tunneling possibility of single-electron current but also the coupling strength of several dopant atoms at the low temperatures.

4. Conclusions

We have investigated single electron tunneling through single and coupling dopant-induced QDs in a heavily n-doped JNT by varying temperatures and bias voltages. We find that the emergence of single-electron peaks at the initial gate voltage is dependent on the increases of the temperature and the bias voltage. There emerge two isolated current peaks below the lower Hubbard band, at which several subpeaks are clearly observed in the double oscillated current peaks due to the coupling of the quantum dots. The energy spacing for both double isolated and double oscillated current peaks is the same as the charge energy of 13.4 meV, which is independent of the gate voltage. The electron transport is dominated by thermally activated hopping at higher temperatures of 30–70 K and by the tunneling in the lower temperatures of 6–20 K. It is possible to adjust the tunneling possibility of single-electron current and the coupling strength of dopant-induced QDs by temperatures and the electric field. This finding demonstrates that silicon JNTs are the promising potential candidates to realize the single dopant atom transistors operating at room temperature.

Acknowledgement

The authors acknowledge Mrs. YunXia Bai, Mr. Jianjun Tang, Mr. Xiaoming Li, and Dr. Liuhong Ma for their supports

in device fabrication.

References

[1] Wang B, Zhang H M, Hu H Y and Shi X W 2018 *Chin. Phys. B* **27** 067402

[2] Bai Z Z, Liu X K, Lian Z, Zhang K K, Wang G H, Shi F F, Pi X D and Song F Q 2018 *Chin. Phys. Lett.* **35** 037301

[3] Afiff A, Samanta A, Udhiarto A, Sudibyo H, Hori M, Ono Y, Tabe M and Moraru D 2019 *Appl. Phys. Express* **12** 085004

[4] Samanta A, Muruganathan M, Hori M, Ono Y, Mizuta H, Tabe M and Moraru D 2017 *Appl. Phys. Lett.* **110** 093107

[5] Diarra M, Delerue C, Niquet Y M and Allan G 2008 *J. Appl. Phys.* **103** 073703

[6] Pierre M, Wacquez R, Jehl X, Sanquer M, Vinet M and Cueto O 2010 *Nat. Nanotechnol.* **5** 133

[7] Bjork M T, Schmid H, Knoch J, Riel H and Riess W 2009 *Nat. Nanotechnol.* **4** 103

[8] Colinge J P, Lee C W, Afzalian A, Akhavan N D, Yan R, Ferain I, Razavi P, O'Neill B, Blake A, White M, Kelleher A M, McCarthy B and Murphy R 2010 *Nat. Nanotechnol.* **5** 225

[9] Ma L H, Han W H, Wang H, Hong W T, Lyu Q F, Yang X and Yang F H 2015 *J. Appl. Phys.* **117** 034505

[10] Tagani M B and Soleimani H R 2014 *Chin. Phys. B* **23** 057302

[11] Sellier H, Lansbergen G P, Caro J, Rogge S, Collaert N, Ferain I, Jurczak M and Biesemans S 2006 *Phys. Rev. Lett.* **97** 206805

[12] Moraru D, Samanta A, Anh le T, Mizuno T, Mizuta H and Tabe M 2015 *Sci. Rep.* **4** 6219

[13] Zhao X S, Han W H, Guo Y Y, Dou Y M and Yang F H 2018 *Chin. Phys. B* **27** 097310